



Short Note

Maskless shaping of gold stud bumps as high aspect ratio microstructures

Rekha S. Pai *, Mark M. Crain, Kevin M. Walsh

Department of Electrical and Computer Engineering, University of Louisville, Louisville, KY 40292, USA

ARTICLE INFO

Article history:

Received 29 March 2010
 Received in revised form 6 August 2010
 Accepted 7 August 2010
 Available online 12 August 2010

Keywords:

Three dimensional
 Microelectrodes
 High surface area
 Microstructures
 Gold stud bump
 Maskless patterning
 Replica molding
 Nanoimprinting
 MEMS

ABSTRACT

Micro/nanoimprinting is a simple and economical way of patterning polymeric structures over large areas. This paper seeks to extend this technique to fabricate three dimensional (3D) metallic microstructures, even in trenches and constrained areas using a flip chip bonder in conjunction with a wire bonder. In this two step process, gold stud bumps were placed first on sputtered metal at appropriate locations using a wire bonder capillary tool. The second step involved flattening of the said gold bump followed by *in situ* restructuring into high aspect ratio microstructures using deep reactive ion etched (DRIE) silicon molds coated with an anti-stiction agent. This process produced microstructures of differing geometries and sizes ranging in height from 1–50 μm and aspect ratios from a low 0.3:1 to as much as 4:1 (with uniformity). The data obtained for 26 different templates, with varying imprint areas, were analyzed and a strong correlation of 1.62X (SD = 0.3) was observed between the force applied and the heights of the resulting microstructures. Final microstructure yield enhancement was around 70% with this technique in comparison to the traditional electroplating through mask approach.

Published by Elsevier B.V.

1. Introduction

Diverse micro electro mechanical system (MEMS) applications ranging from magnetic storage memory and photovoltaic cells to disposable chips for blood analysis would greatly benefit from a reliable and inexpensive method of patterning micro and nano metallic structures. Although traditional microfabrication techniques such as sputtering, evaporation, wet and dry etching used to manufacture these structures are mature, well developed and suitable for mass production, there are certain limitations. These processes were primarily developed for integrated circuit (IC) manufacture and consequently produce low aspect ratio microstructures, are often limited to the use of materials such as semiconductors (mainly silicon) and metals, and capital equipment costs are prohibitive for small scale research laboratories [1,2]. Perhaps, more importantly, a mainstay of all these techniques is the use of UV lithography, which is essentially a two-dimensional process with a limited tolerance for non-planar topography. This severely limits putting down microstructures with any degree of success in constrained areas such as reservoirs and channels found in microchips [3]. Especially effective for MEMS would be a post-processing technique to fabricate 3D metal structures without

any iterations meaning possible new masks and reworking process flows while definitely escalating costs.

Recently metal patterning has been accomplished by non-conventional techniques such as microcasting [4], micromolding [5], Lithographie Galvanoförmung Abförmung (LIGA) [1,6], electric discharge machining [7], selective plating [8], direct nanoimprinting of metal [9,10] and soft lithography [11]. Each of these strategies has its strengths and special features. For example, although LIGA is expensive it yields the highest aspect ratios while soft lithography, microcasting and selective plating allow for 3D free-standing structures but need specialized equipment or chemistry know-how in order to be successful.

A common thread that runs through all these methodologies is the fact that MEMS devices could benefit from the imaginative use of macro techniques e.g., casting, molding and electroplating [2,4,5]. Here we present a two step post-processing fabrication technique utilizing a readily available wire bonder in conjunction with a flip chip bonder or nanoimprinter or any hydraulic die press tool. In the first step gold stud bumps (sphere-like as depicted in Fig. 1A) were placed on sputtered metal at appropriate locations using a wire bonder capillary tool. The second step involved flattening of the said gold bump (Fig. 1B) followed by *in situ* restructuring into three dimensional (3D) high aspect ratio microstructures (Fig. 1C) using deep reactive ion etched (DRIE) silicon molds. In this study we present this new process sequence established by studying the effect of imprint area, force applied, time taken, temperature and perhaps most importantly a

* Corresponding author. Address: US Naval Research Laboratory (NRL), Code 6365 – Materials and Sensors, 4555 Overlook Ave., S.W., Washington, DC 20375-5345, USA. Tel.: +1 202 767 6302; fax: +1 202 767 2087.

E-mail address: rekha.pai@nrl.navy.mil (R.S. Pai).

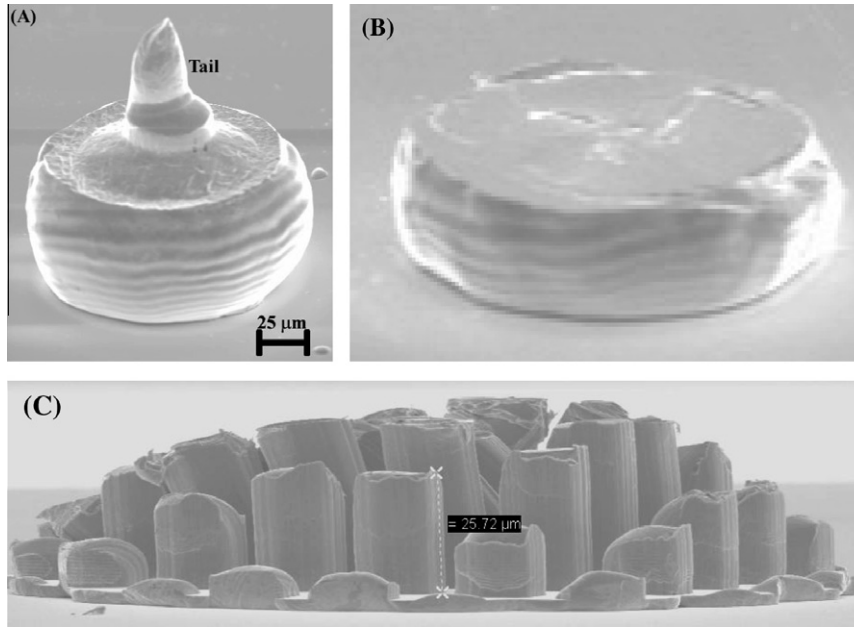


Fig. 1. SEM images of (A) stud bump (B) coined bump and (C) 3D microstructure.

consistent high aspect ratio microstructure after the molding process.

2. Experimental

In this characterization study, the substrates were square pieces of $\langle 100 \rangle$ silicon sputtered with a Cr/Au layer (Cr \sim 30 nm/Au \sim 340 nm). Stud bumps were placed on the test die in a matrix separated in x and y dimensions by \sim 500–600 μm (Fig. 2A) using 1 mil ball bumping gold wire (98% Au, 2% Pd, 2–4% elongation). This ball bumping was accomplished on a model 4524 Kulicke and Soffa (K&S) digital wire bonder with the values: force = 5.0; ball = 5.2; tail = 4.9; chuck temperature = 150 $^{\circ}\text{C}$.

The silicon mold template mask had 26 unique designs with 22 patterns of 5–50 μm squares separated by 5–25 μm streets while the remaining four mold designs consisted of 2.5 and 5 μm circles, polygons and spirals. The square geometries were chosen to quantify critical factors affecting pattern transfer such as the ratio of imprint area to total surface area on the template and resolution. The 50 μm deep molds were fabricated with a standard combination of photolithography and DRIE anisotropic etching (MESC Multiplex ICP, STS plc, Newport, UK) followed by oxygen plasma cleaning. These mold die were then mounted on a handle wafer as a 2×2

array to gain a relatively level surface while imprinting multiple bumps at a time (Fig. 2B). In the next step, a monolayer of an anti-stiction agent perfluoro-octyl-trichlorosilane was evaporated onto the molds at 150 $^{\circ}\text{C}$ in an atmosphere of nitrogen [12].

The microstructures were realized from the stud bumps in a two part process: flattening (or “coining”) the stud bumps followed by imprinting using the micromolds. During the coining, nine stud bumps were flattened with an ultra flat silicon wafer held by the Finetech “Pico” flip chip bonder. The main goal in this step was to press the small length of wire atop a typical ball bump (Fig. 1A) to create a smooth cylindrical profile with a flat top (Fig. 1B). Since the diameter and height of this cylinder would define the volume available for imprinting, the parameters evaluated were maximization of surface area and a smooth, flat top surface. Statistical process control (SPC) was used for optimization of the time, temperature and force required. For the micromolding, four coined bumps were aligned to the 2×2 array of DRIE molds and imprinted with two force values ($F = 25 \text{ N}, 40 \text{ N}$) using the flip chip bonder at 200 $^{\circ}\text{C}$ for 45 s. Total imprint area was the only variable considered while all other pertinent factors such as temperature, time and initial stud bump size or available gold volume ($\sim 3.19 \times 10^{-13} \text{ m}^3$) were kept constant. All metrology measurements were carried out using the SEM, confocal microscope and the profilometer.

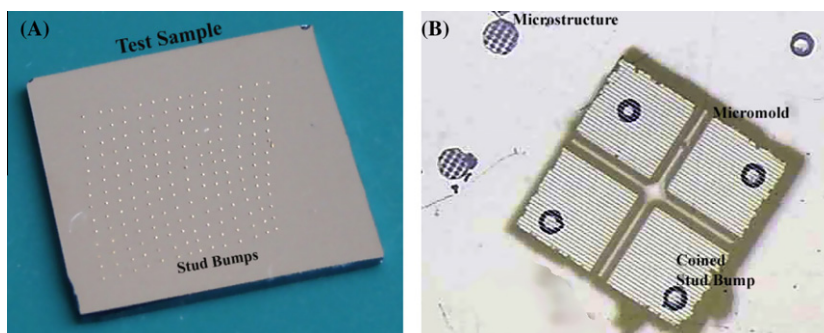


Fig. 2. (A) Test sample die with array of stud bumps and (B) flip chip bonder image showing the alignment of a micromold to four of the coined stud bumps.

3. Results and discussion

A process methodology appropriate for low volume fabrication of high aspect ratio microstructures in constrained areas was successfully developed. In this simple *in situ* technique, the microstructures were realized by reshaping gold stud bumps in two steps – flattening the top surface followed by imprinting the inverse of a microfabricated silicon mold using a flip chip bonder. Alternatively the die could be bumped using methods such as electroplating through masks, soldering and stenciling. The main advantage of the gold stud bump – flip chip approach was the simplicity in processing minus the photolithography step, minimal variation in height of the bump, and the realization of 3D metal microstructures in deep trenches and vias. Scaling up of this process for large area patterning is possible with electroplating in conjunction with a nanoimprinting or hot embossing tool.

Twenty-six mold templates with varying amounts of imprint area were fabricated successfully. A significant finding was that the templates had to be pristine with bare silicon surfaces and sidewalls for the monolayer of the anti-stiction agent to adhere and affect a quick release for satisfactory imprinting. Most importantly, the molds could be reused for imprinting on different substrates for 2–3 days without any significant loss of resolution and/or uniformity in the resultant 3D microstructures.

For the first step of coining, utilization of SPC quickly yielded optimal cylindrical bumps with average height 24 ± 1 and $130 \pm 4 \mu\text{m}$ in diameter under the process conditions: force $F \sim 3.4 \text{ N/bump}$, temperature = 200°C , and time = 45 s. During the micromolding study, total imprint area was the only variable considered. As a means of quantifying the relation between microstructure formation and the 26 different designs involved, a metric R was defined as the percentage of open feature area or imprint area to the total surface area of the mold. Additionally, the molds were classified into groups based on empirical results and theoretical data for further simplification of the analysis.

The results in Table 1 corroborate an association between the open imprint area and the resulting microstructures. High forces ($\geq 40 \text{ N}$) were required for imprinting microstructures with template designs comprised of small openings and wide streets classified as Group I. A typical example of such structures is depicted in Fig. 3 where the imprint pattern was $2.5 \mu\text{m}$ circles.

In Group II, the molds with $R = 10\text{--}23\%$ resulted in uniform ($\pm 1 \mu\text{m}$) microstructures typically $4.4\text{--}12.5 \mu\text{m}$ in height. The structures formed by imprinting with Group II molds had a maximum aspect ratio value of 1.6:1 ($F = 40 \text{ N}$). However, approximately 30% of the gold in the stud bump had not been modified to take on the inverse pattern of the given template at 40 N implying theoretically that higher forces could be potentially applied to increase the aspect ratios.

Overall the microstructures fabricated from Group III micromolds, with approximately 36–49% open imprint area were the best in terms of consistent uniformity, good resolution, planarity and aspect ratios of 1.5:1 obtained at a relatively low force application

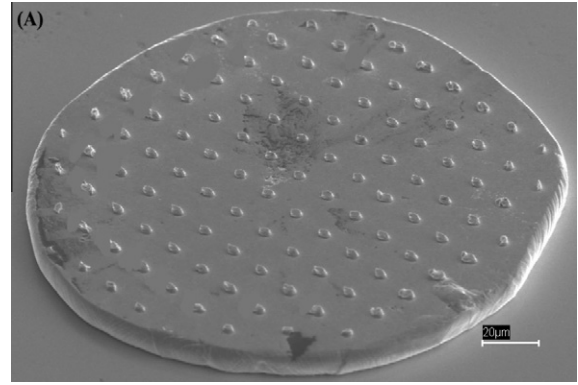


Fig. 3. Examples of Group I microstructures $R \leq 0.08$.

of 25 N. However, in a more interesting development, upon increasing the force being applied to 40 N, it was noticed that after attaining 4:1 aspect ratios, the “micro system” formed takes on a profile reminiscent of a little city or a “MEMStropolis” (Fig. 1C). Theoretical calculations on the amount of gold available and the volume present in the said microstructure confirmed that all the gold had been redistributed during the imprinting. This calculation was later substantiated independently by running the same imprinting experiment on a 0.25 cm thick and 0.5 cm square piece of 99.99% gold providing an infinite volume. Tall (40–60 μm), uniform microstructures were the result of this experiment with aspect ratios as high as 8:1 on application of 100 N (data not shown). These theoretical values and experimental validation lent credence to the theory that the geometry and/or height of the microstructure is limited by the available volume of gold in the ball bump. This constraint was more pronounced in the imprinting with templates classified as Group IV ($R = 56\text{--}64\%$) characterized by wide pillars and small streets. Approximately 10 N of applied force on this group was adequate to produce 30 μm tall free-standing pillars i.e., 2:1 aspect ratios (Fig. 4). However, the “MEMStropolis” profile was a regular feature in the results after 10–15 N.

Continuing the classification of templates and microstructures, Group V contained two micromolds where the imprint area was 70% and 80%, respectively. These mold designs disintegrated on application of $\sim 5 \text{ N}$ or less without yielding any usable structures. Crystalline silicon, the material used in fabrication of the molds has a yield strength of 2800 MPa or $2.8 \times 10^{-3} \text{ N}/\mu\text{m}^2$ approximately twice that of stainless steel making it a great structural material [1]. However, for these molds where the imprint area was large meaning very little unetched silicon, the pressure applied for micromolding was higher than the yield strength thus leading to mold disintegration.

Although majority of the results could be correlated, there were four outliers classified as Group VI. All of these had reasonable R values qualifying them for Groups II, III or IV albeit with thin street widths ($\sim 5 \mu\text{m}$) and each of these could form 6–8 μm tall

Table 1
Summary of results for the formation of microstructures.

Group	No. of mold designs	Imprint percentage R (open/imprint area \div total area) 100	Heights of resulting microstructures @ applied force (N)		
			$\leq 10 \text{ N}$	$\approx 25 \text{ N}$	$\geq 40 \text{ N}$
I	4	0–8%	No	No	Ok
II	8	10–23%	Ok	4.4–12.5 μm uniform	6–16 μm uniform
III	5	36–49%	Ok	20–24 μm uniform	4–40 μm non-uniform
IV	3	56–64%	30 μm uniform	4–40 μm non-uniform	No
V	2	>71%	No	No	No
VI	4	25%, 33%, 43% and 66%	Ok	6–8 μm uniform	No

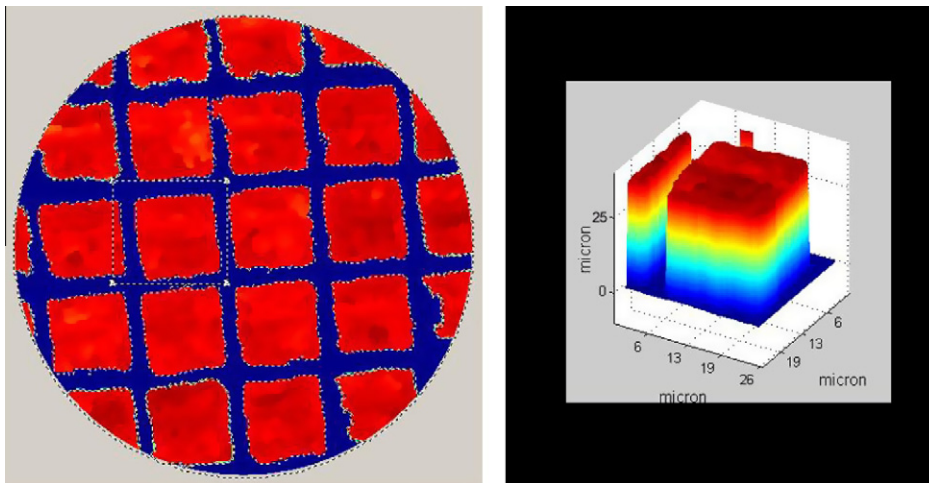


Fig. 4. Confocal microscopy image of a uniform 3D structure ($R = 0.56$).

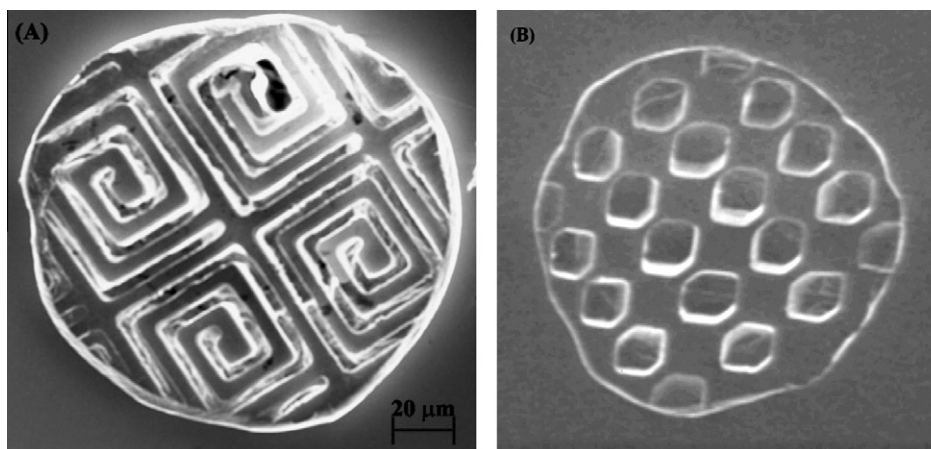


Fig. 5. SEM images (top view) of Group VI microstructures (A) spirals and (B) hexagons.

microstructures (Fig. 5) on application of force = 10–30 N. However, the molds disintegrated at 15 N in case of the spiral and hexagon patterns, and 30 N in the square designs. In addition, problems such as sticking/breaking of the mold and shearing off of the stud bumps were noticed during the imprinting process at low force values. These results might be due to the critical dimensions of the patterns i.e., thin street widths and more importantly the small aperture sizes (5–7 μm) leading to incomplete polymer removal from the sidewalls during ashing consequently making it difficult to get an even layer of anti-stick coating.

The results in Table 1 suggest a relation between imprint area, force applied and microstructures formed. Uniform structures could be fabricated with all of the Groups II and III molds where the open imprint area ratio was 10–59%. The heights of the microstructures formed at 25 and 40 N from these molds i.e., 1.6 times increase in force, were compared and found to increase anywhere between 1.28X–2.05X (Avg. = 1.62X, SD = 0.27) implying good correlation between the force applied and the heights of the resulting microstructure. The slight variation in heights could be attributed to other variables such as time and temperature, area of stud bump to be imprinted, purity of gold used, shape of structures etc. all of which have not been studied in this research.

A practical example of this processing technique involved its use to fabricate high surface area electrodes/reactors for coulometry and anodic stripping voltammetry in LOC devices [3,13]. Previ-

ously we have employed electroplating through resist masks to fabricate a trio of 30 μm diameter and $\sim 15 \mu\text{m}$ high 3D pillar-like nickel electrodes for the detection of carbohydrates and sugars [14]. Direct comparison of the two fabrication process flows showed a 70% improvement in product yield for this new method. Furthermore, significant time and cost savings were realized production-wise with the modified stud bump approach to make finer and as a result higher surface area 3D microelectrodes [3] due to the absence of photolithography steps. Another exciting area of applicability currently under investigation is selective surface modifications for bump restructuring to promote stenciling in adhesive and flip chip bonding.

4. Conclusions

In summary a simple and inexpensive process methodology appropriate for patterning metal to create 3D micro/nanostructures even on constrained surfaces has been developed. The primary advantage in this technique of reshaping gold ball bumps by imprinting with silicon micromolds stems from the ability to construct multiple geometry and/or type high surface area structures in one step (e.g., spirals, circles and squares in one mold). Using this novel process, microstructures of differing geometries and sizes ranging from 1–50 μm with the smallest imprint

~400 nm were achieved. Aspect ratios from a low 0.3:1 to as much as 4:1 (with uniformity) were manufactured in a relatively easy manner by choosing an appropriate combination of micromolds used and applied force. Uniform microstructures ($\pm 3 \mu\text{m}$ variation in height across the $100 \mu\text{m}$ wide stud bump) could be fabricated easily with the application of 25–40 N on micromolds possessing open imprint area ratios in the range 10–59%. The heights of the resultant microstructures were found to increase an average of 1.62X (SD = 0.3) for the 1.6 times increase in force from 25 to 40 N suggesting a good correlation between the force applied and the heights of the resulting microstructures. The only constraint in fabricating 10:1 or higher aspect ratio structures with uniformity was the available raw material in the gold stud bump. Nevertheless, the ability to create 3D structures reproducibly especially in trenches is valuable for many MEMS devices. In production terms, yield improvements were as high as 70% compared to selective electroplating. Moreover, this novel approach afforded significant savings in time, manpower and most importantly a positive cost-benefit ratio.

Acknowledgements

Financial support for this work was provided by the Department of Energy through Grant # 4-64111-01-0950. Rekha S. Pai was funded by a University of Louisville fellowship during this project.

References

- [1] M.J. Madou, *Fundamentals of Microfabrication*, first ed., CRC Press, Boca Raton, FL, 1997.
- [2] A.B. Frazier, R.O. Warrington, C. Friedrich, *IEEE Trans. Ind. Electron.* 42 (5) (1995) 423–430.
- [3] R.S. Pai, K.M. Walsh, M.M. Crain, T.J. Roussel Jr., D.J. Jackson, R.P. Baldwin, R.S. Keynton, J.F. Naber, *Anal. Chem.* 81 (12) (2009) 4762–4769.
- [4] G. Baumeister, K. Mueller, R. Ruprecht, J. Hausselt, *Microsyst. Technol.* 8 (2) (2002) 105–108.
- [5] E.C. Hagberg, J.C. Scott, J.A. Shaw, T.A. von Werne, J.A. Maegerlein, K.R. Carter, *Small* 3 (10) (2007) 1703–1706.
- [6] M.W. Borner, M. Kohl, F.J. Pantenburg, W. Bacher, H. Heln, W.K. Schomburg, *Microsyst. Technol.* 2 (3) (1996) 149–152.
- [7] D. Reynaerts, P.-H. Heeren, H.V. Brussel, *Sens. Actuators, A: Phys.* 60 (3) (1997) 212–218.
- [8] S. Konishi, K. Honsho, M. Yanada, I. Minami, Y. Kimura, S. Ikeda, *Sens. Actuators, A: Phys.* 103 (1) (2003) 135–142.
- [9] L.J. Guo, *Adv. Mater.* 19 (4) (2007) 495–513.
- [10] H.L. Chen, S.Y. Chuang, H.C. Cheng, C.H. Lin, T.C. Chu, *Microelectron. Eng.* 83 (6) (2006) 893–896.
- [11] R.J. Jackman, S.T. Brittain, A. Adams, M.G. Prentiss, G.M. Whitesides, *Science* 280 (5372) (1998) 2089–2091.
- [12] M. Beck, M. Graczyk, I. Maximov, E.-L. Sarwe, T.G.I. Ling, M. Keil, L. Montelius, *Microelectron. Eng.* 61–62 (2002) 441–448.
- [13] T.J. Roussel Jr., R.S. Pai, M.M. Crain, D.J. Jackson, L. Sztaberek, K.M. Walsh, J.F. Naber, R.P. Baldwin, R.S. Keynton, 3D microelectrodes for coulometric screening in microfabricated lab-on-a-chip applications, in: 4th IEEE-EMBS Conference on Microtechnologies in Medicine and Biology, Okinawa, Japan, 2006, pp. 233–235.
- [14] R.S. Pai, T.J. Roussel Jr., M.M. Crain, D.J. Jackson, R.P. Baldwin, R.S. Keynton, J.F. Naber, K.M. Walsh, Electroplating for three dimensional lab on a chip electrodes and microstructures, in: 2nd Joint EMBS-BMES Conference, Houston, TX, 2002, pp.1663–1664.